

Preparation and Self-assembly of Chiral Porphyrin Diads on the Gold Electrodes of Quartz Crystal Microbalances: A Novel Potential Approach to the Development of Enantioselective Chemical Sensors

Roberto Paolesse,^{*,[a]} Donato Monti,^[a] Laura La Monica,^[a] Mariano Venanzi,^[a] Antonella Froiio,^[a] Sara Nardis,^[a] Corrado Di Natale,^[b] Eugenio Martinelli,^[b] and Arnaldo D'Amico^[b]

Abstract: Porphyrin diad **1** was synthesized by reaction of the acyl chloride of porphyrin **2** and *trans*-1,2-dithiane-4,5-diol. The Co complex of this diad was studied as a potential enantioselective receptor for chiral recognition in solution and in the solid state. In solution both enantiomers of limonene induce significant changes in the visible and circular dichroism (CD) spectra of [Co₂(**1**)], while a different behavior is observed in the case of the enantiomeric pair of *trans*-1,2-diaminocyclohexane. A different efficiency of [Co₂(**1**)] chiral

recognition is obtained for these compounds, with a remarkable degree of enantiodiscrimination observed in the case of limonene. Self-assembled monolayers of [Co₂(**1**)] were deposited onto the gold electrodes of quartz crystal microbalances to be used as sensing materials of nanogravimetric sensors operating in the gas phase. The enantio-

discrimination properties of these sensors towards the enantiomeric pairs of chiral analytes have been studied. While in the case of analytes bearing donor ligand atoms we did not observe a remarkable enantioselectivity, a significant degree of chiral discrimination was observed in the case of limonene; this result is particularly encouraging for the potential development of enantioselective chemical sensors for use in an array configuration.

Keywords: enantiomeric recognition • monolayers • porphyrinoids • self-assembly • sensors

Introduction

The modification of inorganic surfaces by chemisorption of organic compounds is an interesting approach to the fabrication of hybrid organic/inorganic materials, the properties of which are almost unexplored.^[1] When adequately developed, these materials could have a tremendous impact in the development of technologies in which the versatility of organic compounds is a requirement.^[2]

One of the fields in which this goal seems to be close to realization is the development of chemical sensors.^[3] In these devices interactions at the sensor surface are clearly of critical importance: the possibility of a direct bond between the sensing material and the transducer surface can greatly improve sensor performance. For example, it can allow both

an enhancement of the selectivity properties and an optimization of the transduction mechanism. Of course some important limitations should be taken into account, such as the low saturation limit of the resulting sensor. This aspect, however, is not necessarily a drawback, but rather represents an advantage in the presence of low concentrations of analytes.

Among the different molecules proposed as sensing materials we have been particularly focused on porphyrins.^[4] In the last few years we have developed sensor arrays composed of quartz crystal microbalances (QCMs) coated with metal complexes of porphyrins for the analysis of volatile organic compounds (VOCs).^[5] Metalloporphyrins have been particularly useful in these applications, because of their stability and their versatility as binding agents.^[6] Various examples of the self-assembly of porphyrins onto inorganic surfaces have been reported in the literature.^[7] We have been able to functionalize the QCM by depositing self-assembled monolayers of thiol-substituted porphyrins onto the gold electrodes of the QCM disks; the resulting sensors showed satisfying sensing properties for the detection of VOCs.^[8]

These promising results led us to explore a further step in the exploitation of self-assembled, functionalized QCMs. In the previously developed QCMs, single porphyrins were

[a] Dr. R. Paolesse, Dr. D. Monti, L. La Monica, Prof. M. Venanzi, A. Froiio, S. Nardis
Dipartimento di Scienze e Tecnologie Chimiche
Università di Roma Tor Vergata
Via della Ricerca Scientifica, 00133 Rome (Italy)
Fax: (+39) 6-72594328
E-mail: roberto.paolesse@uniroma2.it

[b] Prof. C. Di Natale, E. Martinelli, Prof. A. D'Amico
Dipartimento di Ingegneria Elettronica
Università di Roma "Tor Vergata", 00133 Roma (Italy)

chemisorbed onto the electrode surface; our present approach involves the deposition of a chiral porphyrin diad in order to create a more complex receptor for the recognition of VOCs. Our goal is to test such a device for enantiomeric recognition. This aspect, though particularly challenging, is remarkably important when applied to the analysis of real matrices, as enantiomers are chemically and physically identical in an achiral environment, differing only by the spatial arrangement of their elements. In biological systems enantiomeric discrimination is performed by interaction of chiral molecules with enantiomerically pure receptors;^[9] the progress of supramolecular chemistry has given a great impulse to the development of a similar host–guest concept with simple molecular systems, and several elegant systems have been proposed to enhance chiral discrimination in solution.^[10] A similar host–guest approach has been used in analytical chemistry to obtain discrimination and separation of mixtures of enantiomers by GC and HPLC chromatographic methods.^[11] This has generally been achieved by using stationary phases functionalized with chiral receptor sites. On the other hand, while a huge number of chemical sensors have been developed, only a few examples have been reported in which chiral discrimination is performed by chemical sensors.^[12] In these studies the researchers used sensing materials composed of an inert matrix into which chiral receptors were dispersed; these materials have been derived from those exploited as stationary phases in the GC technique.

However in the case of some real application, such as the aroma of foods, in which chiral compounds often represent a fundamental component of the blend, the use of conventional analytical methods is usually hampered by the overwhelming complexity of their chemical composition.^[13] In this case, mimicking the human nose, which is able to discriminate between the enantiomers of limonene simply on the basis of their different smell, constitutes a desirable goal.

Since the seminal paper of Persaud and Dodd,^[14] artificial olfaction has been achieved by using an array of different chemical sensors, each with different selectivity properties towards the various chemical species present in the gaseous phase.^[15] In this way the whole sensor array gives information related to the bulk environment, and the subsequent data analysis interprets this information on the basis of the chemical composition.^[16] An advantageous feature of such a system is that the absolute selectivity of each individual sensor is not required.^[17]

Using this approach, our long-term goal is to develop chemical sensors with enantiomeric recognition properties towards some classes of chiral analytes. These devices will be designed for sensor array exploitation, in order to develop an electronic nose devoted to the analysis of real matrices, in which chiral analytes can play an important role.

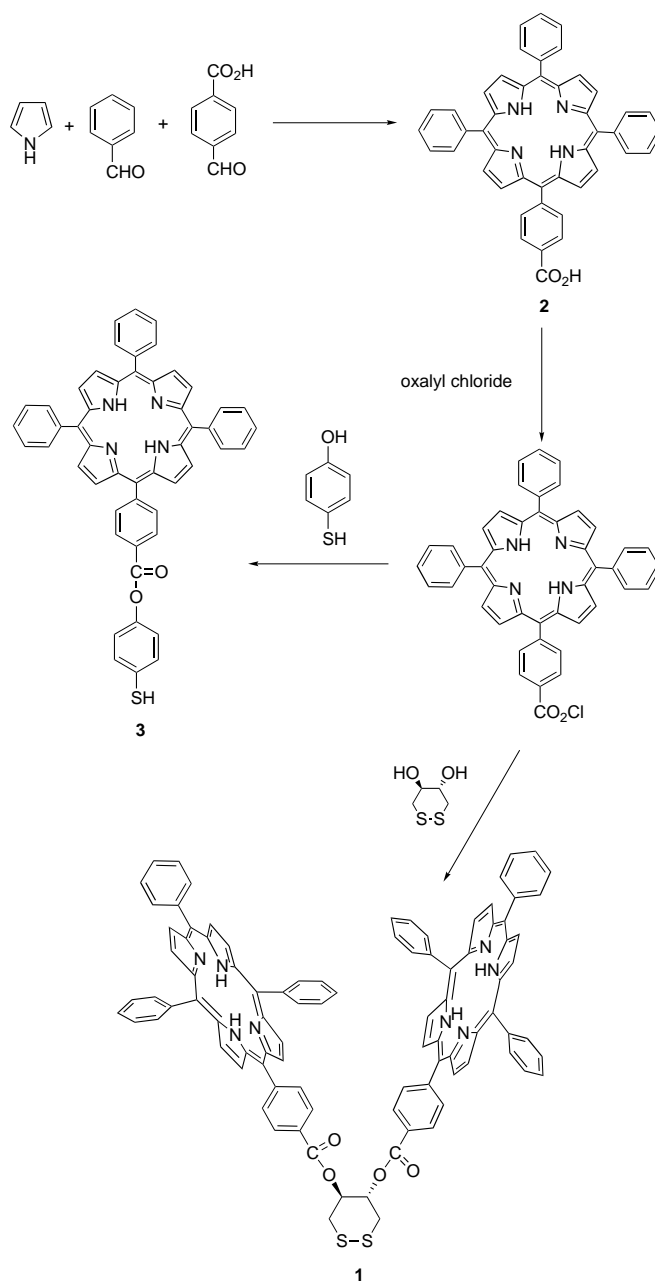
We decided to first explore the use of QCMs functionalized by monolayers of a chiral receptor directly linked to the sensor surface. This method is particularly appealing, because it could avoid the occurrence of spurious interactions as a result of the bulk of the sensing materials; this would greatly improve their recognition performance.

In this work we present the synthesis of a chiral porphyrin diad suitable for deposition as a self-assembled monolayer

onto the gold pad of QCM sensors. The binding behavior of such a diad was first tested in solution, while its sensing and chiral discrimination properties toward some enantiomeric pairs of chiral compounds were measured by QCM sensors.

Results and Discussion

Synthesis and binding studies in solution: The porphyrin diad **1** was prepared following the synthetic pathway depicted in Scheme 1. Porphyrin **2** reacted with oxalyl chloride in dichloromethane solution to give the corresponding porphyrin acyl chloride; this intermediate was then treated with dithiane to afford **1** in satisfactory yield. In the same way, **3**



Scheme 1. Synthetic pathway to **1**.

was prepared by reaction of the intermediate porphyrin acyl chloride with thiophenol. Co complexes of **1** and **3** were obtained by following standard metalation procedures.^[18] We chose Co as the coordinated metal, because Co porphyrins have been successfully used as sensing materials in electronic nose applications.^[4]

The UV-visible spectrum of the [Co₂(**1**)] diporphyrin receptor features two bands in the Soret region at 435 and 412 nm, in a 1:4 intensity ratio. The invariance of the spectrum profile over a wide concentration range (1×10^{-7} – 5×10^{-5} M) safely rules out the occurrence of an aggregation effect on the observed phenomenon. On the basis of the spectral profile the occurrence of an equilibrium between two different conformations, one open and one closed, can be hypothesized. In the open conformation the porphyrin macrocycles are probably held apart, resulting in a noninteracting, energetically monomer-like structure, which generates the Soret band at 412 nm. In the closed structure, the two macrocycles are probably held in a J-type conformation, resulting in a red-shifted, somewhat broadened absorption band at 435 nm.^[19]

The addition of *S*-(–)- or *R*-(+)-limonene to a solution of [Co₂(**1**)] causes dramatic changes in the UV-Visible spectra of the receptor. Figure 1 shows the peculiar evolution of the

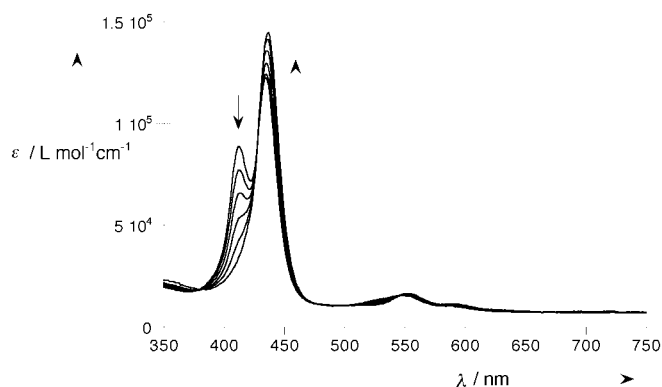


Figure 1. UV-visible spectral changes (Soret band selected region) of [Co₂(**1**)] (1.8×10^{-5} M), at various concentrations of *S*-(–)-limonene in CHCl₃. The arrows indicate the changes upon increasing limonene concentration.

spectral pattern (i.e. the two Soret bands at 412 and 435 nm) into a new, red-shifted band at 437 and 438 nm for *S*-(–)- and *R*-(+)-limonene, respectively. A significant hyperchromic effect is also present. A red shift of the two Q visible bands is also evident upon limonene addition. These results can be explained in terms of inclusion of the unsaturated species within the receptor walls, as a consequence of π – π interaction between the limonene double bonds and the aromatic system of the porphyrin platforms.^[20] The overall association constant values K , for the binding of the limonene enantiomers to the diporphyrin receptor, can be calculated from the spectral changes (Figure 2). The experimental points can be fitted by a 1:1 binding curve.^[21] The preference for the *S*-(–) over the *R*-(+) enantiomer, demonstrated by their relative K values 6200 and 1600 M^{-1} , respectively, is in close agreement with that observed in the solid-state experiments (vide infra).

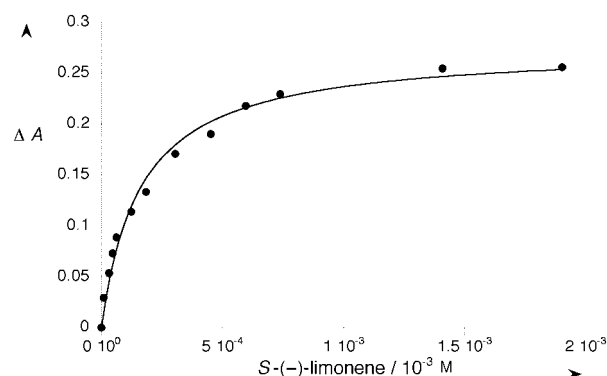


Figure 2. Titration plot ($\lambda = 437$ nm) of [Co₂(**1**)] (1.8×10^{-5} M), at various concentrations of *S*-(–)-limonene in CHCl₃. The points are experimental and the curve is calculated for 1:1 complex formation (see text).

Analogous experiments carried out with cyclohexene, a related olefinic structure bearing only one double bond, showed a much weaker interaction ($K < 10 \text{ M}^{-1}$); this supports the above-given hypothesis. Evidently, the two unsaturated bonds of limonene act cooperatively, resulting in a stronger interaction.

Parallel circular dichroism (CD) spectroscopic experiments gave further compelling evidence for the inclusion of the chiral analytes within the receptor walls. The [Co₂(**1**)] diporphyrin system features an intense, negative dichroic band ($[\theta] = 1.5 \times 10^4 \text{ deg cm}^2 \text{ dmol}^{-1}$) at 440 nm, (2×10^{-5} M chloroform solution, Figure 3), along with a weaker ($[\theta] = 1.2 \times 10^3 \text{ deg cm}^2 \text{ dmol}^{-1}$) negative band centered at 415 nm. The red-shifted absorption probably corresponds to the closed, J-like conformation, whereas the less intense band arises from the open structure.

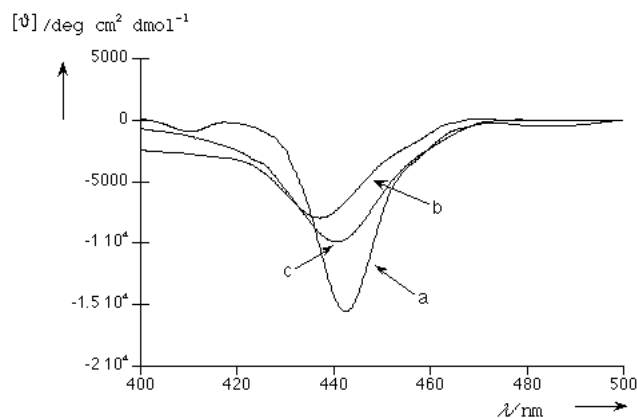


Figure 3. a) CD spectra of [Co₂(**1**)] (1.8×10^{-5} M, CHCl₃, 298 K); b) in the presence of *R*-(–)-limonene 5.0×10^{-3} M; c) in the presence of *S*-(+)-limonene 5.0×10^{-3} M.

The addition of an excess of *S*-(–)-limonene promotes a decrease of the CD amplitude ($[\theta] = 9.8 \times 10^3 \text{ deg cm}^2 \text{ dmol}^{-1}$). Furthermore, the addition of *R*-(+)-limonene results in an even more pronounced decrease of the CD band intensity, up to $7.8 \times 10^3 \text{ deg cm}^2 \text{ mol}^{-1}$. This finding can be explained by the formation of supramolecular complexes that are characterized by a lower degree of ellipticity. Remarkably, the CD-coupled band at 415 nm,

disappears upon the formation of a limonene–[Co₂(**1**)], in a close analogy to that observed in the UV-visible spectroscopic studies. This finding corroborates the hypothesis that the guest is sandwiched within the porphyrin platforms of the receptor.

The larger CD hypochromic effect observed in the case of the *R*-(+) enantiomer would indicate that the formation of the inclusion complex occurs with higher structural reorganization (i.e. unfavorable cage complementarity). This lack of pre-organization of the structure would constitute an insurmountable drawback in the solid-state interaction, dictating the preference for the *S*-(-) enantiomer.

UV-visible spectroscopic studies were also carried out in the case of *trans*-*R,R*-(-) and *trans*-*S,S*-(+)-1,2-diaminocyclohexane (+/- DACy). Spectral changes are exhibited by the diporphyrin receptor upon nitrogen-to-metal coordination, in close analogy to those observed in the case of the interaction with the limonene enantiomers. A striking difference resides in the Soret bands of the resulting DACy–[Co₂(**1**)] supramolecular complexes, which feature blue-shifted maxima at 431 nm (Figure 4). This finding implies the formation of a complex in which the porphyrin platforms are held in a geometry that would probably be tighter than that achieved by the complexes with limonenes.

The [Co₂(**1**)] receptor features a rather small degree of enantioselectivity toward the binding of *trans*-*R,R*-(-) and *trans*-*S,S*-(+)-1,2-diaminocyclohexane stereoisomers, *K* being 3.3 and 2.8 × 10⁴ M⁻¹, respectively, which corresponds to a ratio as small as 1.2.^[22]

Thin-film depositions: Porphyrin monolayers were deposited onto gold surfaces by following two different procedures. In the first approach the diad was first synthesized and then deposited onto the gold surface by dipping the substrate into a solution of **1** in chloroform. In the second approach the gold surface was first modified by chemisorption of dithiane; this functionalized surface was then dipped into a solution of the porphyrin acyl chloride in CH₂Cl₂ to obtain the diad in situ.

We took this latter approach to deposit monolayers of the monomeric 4-Co-5'-(4'-carboxyphenyl)-10',15',20'-triphenylporphyrinyl]-1-mercaptobenzene ([Co(**3**)]). In this case the surface was modified by adsorption of thiophenol and then the surface was treated with porphyrin acyl chloride to obtain the relative porphyrin monolayer. We used [Co(**3**)] to compare its properties with those of [Co₂(**1**)] in the subsequent sensor measurements.

We modified the gold electrodes present on both sides of the QCMs, then used for sensing measurements, and transparent gold layers deposited on glass substrates. The formation of monolayers was monitored by the frequency change of the QCMs, caused by the chemisorption

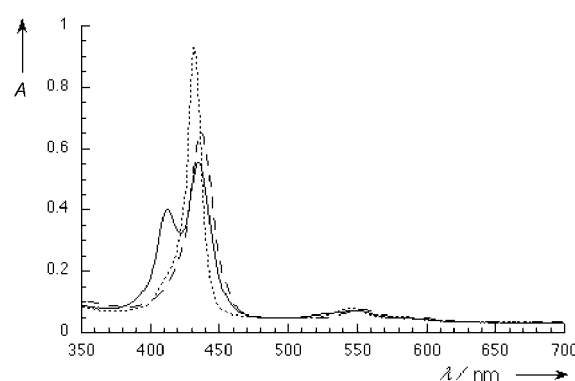


Figure 4. UV-visible spectral changes of [Co₂(**1**)] (1.8×10^{-5} M, in CHCl₃; continuous line) upon addition of *S*-(-)-limonene (3.6×10^{-3} M; dashed line), and *trans*-1,2-DACy (1.2×10^{-4} M; dotted line).

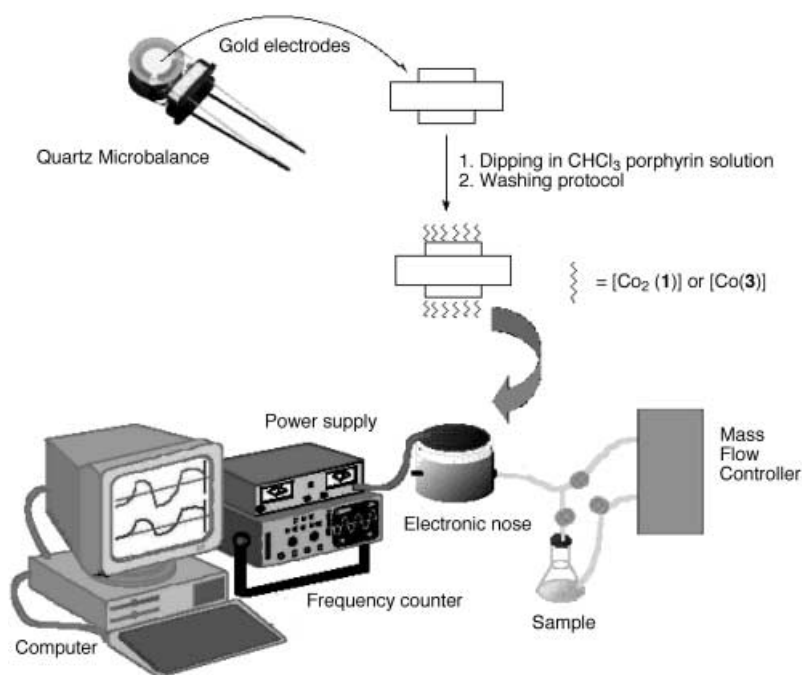
of [Co₂(**1**)] or [Co(**3**)], or by recording the visible spectrum in the case of glass substrates. The experimental set up for QCM measurements is reported in Scheme 2.

The amount of the sensing material deposited on the QCMs can be determined from the change in the resonating frequency of the quartz. In the absence of viscoelastic effects, the relationship between quartz frequency shift and adsorbed mass is, in a first approximation, linear, as described by the Sauerbrey Equation [Eq. (1)].^[23] The constant *K_q* is given by Equation (2), in which *f₀* is the fundamental frequency of the QCM, *v_s* is the sound velocity on the quartz, *A* is the QCM area, and *ρ_c* is the density of the deposited molecular film.

$$\Delta f = -K_q \Delta m \quad (1)$$

$$K_q = \frac{2f_0^2}{v_s \rho_c A} \quad (2)$$

Equation (1) holds only if the viscoelastic effect can be neglected. This condition depends on the thickness of the



Scheme 2. Experimental set up for QCM measurements.

adsorbed mass and it may be assumed valid in case of a molecular monolayer.

The K_q constant can be either calculated from Equation (2) or determined experimentally for each QCM by deposition of a known amount of mass onto the quartz surface. We followed this latter procedure and obtained a value of $1.00(\pm 0.02)$ Hz ng⁻¹.

After deposition of [Co₂(**1**)], we obtained a frequency shift of about 500 Hz in the case of the two-step approach, while the single-step method afforded smaller changes, with a frequency shift around 350 Hz. All these depositions were carried out in triplicate, by dipping three different QCMs into the same organic solution of the diad, and the frequency changes obtained were reproducible within 5%.

Longer deposition times did not increase the frequency changes, while shorter times gave smaller values, indicating incomplete coverage of the gold surface.

According to Equation (1), and considering the measured quartz constant, the amount of [Co₂(**1**)] self-assembled onto the gold electrode of the QCM may be estimated to be in the $500(\pm 10)$ ng range. From this value we can calculate the moles and then the number of the molecules deposited onto the quartz surfaces. For a total gold surface of 1.25 cm² (considering both sides of the QCM), an area of 66 Å² per molecule can be estimated. Considering that a single porphyrin molecule has an area of 225 Å², the value we obtained is even lower than that expected for a porphyrin ring oriented perpendicular to the surface. However, previous STM measurements showed that the electrode surface is very rough, with the characteristic grain structure of evaporated gold.^[24] This should negatively influence the accuracy of the determination of the real surface area, and can explain the small value estimated. In fact, if we consider the gold crystallites as hemispheres, we can estimate the real surface from simple geometrical considerations by the relation $S_{\text{real}} = 2\pi r^2 S_{\text{geometrical}} / \pi r^2$, in which $2\pi r^2$ is the surface of a hemisphere and $S_{\text{geometrical}} / \pi r^2$ is the total number of hemispheres. From this relation we obtain that $S_{\text{real}} = 2S_{\text{geometrical}}$, without considering the interstitial space between the hemispheres. As a consequence the area per molecule assumes the more reasonable value of more than 130 Å². On the other hand we have to exclude the possibility that the high mass value could be caused by the presence of further porphyrin diads aggregated onto the layer directly bound to the surface. It is well known, in fact, that porphyrins show a strong tendency to aggregation by π - π stacking of their aromatic rings.^[21a, 25] However these molecules are linked by weaker interaction and, if present, they are effectively removed by the washing protocol adopted after the deposition. To control the efficiency of the procedure we measured the resonating frequency of the QCMs before and after each washing step and we detected no variation after the first cleaning treatment. To further check this point we deposited additional layers of the porphyrin diad by a spray-coating technique onto one of the [Co₂(**1**)]-functionalized QCMs.^[4f] After drying the surface with an N₂ stream, we treated this quartz by the usual washing protocol; after this treatment we obtained the starting resonating frequency value for the [Co₂(**1**)] QCM, indicating that the further layers were completely removed by the cleaning protocol. The same

experiment was carried out with a bare quartz and we obtained the same result, confirming that the cleaning procedure removes all the porphyrin diads not chemisorbed on the gold surface.

These results seem to indicate complete coverage of the surface and a close-packing of the molecules, with the porphyrin rings oriented in an almost perpendicular fashion to the gold surface.

We also have to consider the possibility of the occurrence of aggregation phenomena among the macrocycles linked to the surface; this phenomenon is generally not advantageous for sensing applications, as the presence of porphyrin stacking does not allow an optimal interaction of the volatile analytes with the macrocycles.

In the case of porphyrins, optical spectroscopy is a powerful method for the investigation of aggregation and coordination phenomena.^[25, 26] For this reason we deposited monolayers of [Co₂(**1**)] onto transparent gold surfaces, and the optical spectrum obtained is shown in Figure 5.

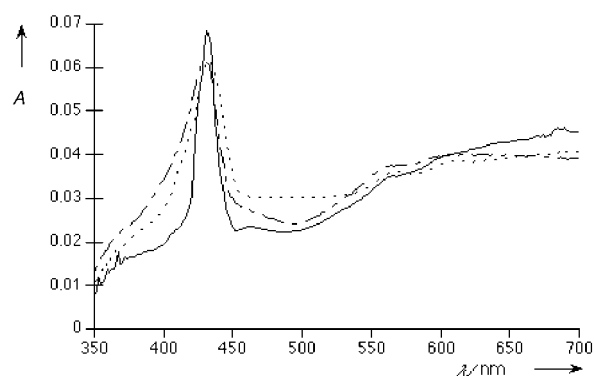


Figure 5. Visible spectra of [Co₂(**1**)] deposited on gold transparent layer (dashed line), upon addition of triethylamine vapors (dotted line), upon addition of limonene vapors (continuous line).

In the solid state the Soret band is centered at 432 nm and the splitting observed in solution is not present; however the band is somewhat broadened and, as a consequence, the less intense, red-shifted band may not be resolved. Exposure of the functionalized glass substrates to different volatile compounds demonstrated the interactions of the porphyrin layers with these analytes. In the case of triethylamine (Figure 5) there is a small red shift of the Soret band, indicating the coordination of the amine to the metal center. It is interesting to note that this red shift is analogous to that observed in solution for Co porphyrin complexes.^[26] To study the influence of the metal coordination on the sensing properties we performed the same experiment with VOCs without donor atoms, such as limonene. In this case a significant sharpening of the Soret band was observed, without significant shift of the absorption band. This feature is similar to that observed in solution, supporting a similar binding mechanism in the recognition phenomenon (Figure 5).

QCM studies. We studied the sensing performance of the functionalized QCMs described in the previous section towards the detection of VOCs (for the experimental set up

see Scheme 2). For these studies we used eight different QCMs housed in a 10 mL measurement chamber: two of them were modified with **3**, and four of them with [Co₂(**1**)], deposited by the two different approaches. We used each sensing material in duplicate in order to test the reproducibility of the performances. The other two positions in the array were occupied by a bare QCM, and by a [Co(tpp)] (tpp = tetraphenylporphyrin) spray-coated QCM. In this way all of the sensors were exposed to the analytes in the same conditions, allowing for a direct comparison of the performances of the self-assembled QCM with both a bare QCM, and with a sensor currently used in the electronic nose.^[4]

In the first phase, we carried out studies on the sensitivity of the QCMs towards simple molecules, such as triethylamine. In this case we observed a good sensitivity of the sensors toward this analyte, but we obtained saturation of the self-assembled QCMs in all cases, even in the presence of very low concentrations of triethylamine. This low saturation limit is not unexpected in the case of a sensing material monolayer; it is important to note that the saturation value is in good agreement with the theoretical value obtained from Equation (1), considering a 1:1 binding stoichiometry between each Co–porphyrin and triethylamine. At higher concentrations of the analyte we observe an increase of the sensor responses, due in this case to the deposition of further layers of the analyte on the QCM surface, as expected for a BET-like (BET = Brunauer–Emmet–Teller) behavior.^[27]

We then studied sensor responses towards some enantiomeric pairs of chiral compounds, namely limonene, menthol, 1,2-DACy, and ephedrine; we chose compounds with similar molecular structure and with or without donor atoms, in order to determine the importance of metal coordination in the *enantiosensing* recognition process.

The sensor array was exposed to saturated vapors of each compound. The measurement of each isomer was performed five times and the results obtained are reported in Table 1. Surprisingly, with the menthol, 1,2-DACy, and ephedrine enantiomeric pairs, we did not obtain significant differences in the sensor responses; the frequency change ratios being close to one. This finding can be explained by considering the saturation limit of each sensor, calculated as reported in the previous section. We obtained, in fact, a [Co₂(**1**):analyte binding stoichiometry of 1:2 for all of these compounds, probably indicating that the two Co–porphyrins behave independently in the coordination of the analytes to the metal centers.

Remarkably, a significant chiral discrimination is observed in the case of limonene, a structure closely related to menthol, the most evident difference being the lack of an oxygen donor site. The $\Delta F_{(-)}/\Delta F_{(+)}$ value for the enantiomeric pair was as large as 3.6, and this result nicely confirms what we observed in solution. It is interesting to note that we obtained a binding stoichiometry of about 1:3 for *S*-limonene, indicating that a complex binding mechanism involving π – π interaction is probably in operation, as is the case in solution.

When we exposed the QCMs to a racemic mixture of limonene, we obtained sensor responses of intermediate value between the two pure enantiomers. It is also worth mention-

Table 1. Average sensor responses of QCM modified with different self-assembled monolayers of porphyrins upon exposure to enantiomeric pairs of chiral VOCs.

Sensing material	analyte	ΔF [Hz]	$\Delta F_{(-)}/\Delta F_{(+)}$	
3	<i>R,S,R</i> (–)-menthol	48 (±3)	1.1	
	<i>S,R,S</i> (+)-menthol	42 (±3)		
	<i>S</i> (–)-limonene	60 (±5)	1.1	
	<i>R</i> (+)-limonene	55 (±4)		
	<i>R,R</i> (–)-1,2-DACy	51 (±4)	1.1	
	<i>S,S</i> (+)-1,2-DACy	45 (±3)		
	<i>R,S</i> (–)-ephedrine	20 (±1)	1.1	
	<i>S,R</i> (+)-ephedrine	22 (±3)		
	1 (two step)	<i>R,S,R</i> (–)-menthol	53 (±4)	0.8
		<i>S,R,S</i> (+)-menthol	62 (±6)	
<i>S</i> (–)-limonene		233 (±9)	3.6	
<i>R</i> (+)-limonene		65 (±3)		
<i>R,R</i> (–)-1,2-DACy		69 (±7)	1.2	
<i>S,S</i> (+)-1,2-DACy		59 (±5)		
<i>R,S</i> (–)-ephedrine		61 (±4)	1.4	
<i>S,R</i> (+)-ephedrine		44 (±7)		
1 (one step)		<i>R,S,R</i> (–)-menthol	72 (±6)	0.9
		<i>S,R,S</i> (+)-menthol	84 (±3)	
	<i>S</i> (–)-limonene	108 (±7)	2.1	
	<i>R</i> (+)-limonene	51 (±5)		
	<i>R,R</i> (–)-1,2-DACy	58 (±3)	1.1	
	<i>S,S</i> (+)-1,2-DACy	51 (±4)		
	<i>R,S</i> (–)-ephedrine	58 (±6)	1.2	
	<i>S,R</i> (+)-ephedrine	48 (±2)		

ing that QCMs modified with **3** did not show significant differences between racemate and enantiomers, as expected in the absence of chiral discrimination.

Because limonene is the more volatile among the different compounds tested, we exposed the sensor array to cyclohexene-saturated vapors to exclude the different volatility as the reason for the higher sensor responses; in this case the frequency shifts were significantly low, excluding saturation effects in the chiral discrimination of limonene.

Conclusion

Diad **1** was straightforwardly synthesized starting from dithiane and **2**. This diad was used to modify the gold surface present on quartz crystal microbalances (QCMs) by following two different approaches. The formation of the organic layer was monitored by the frequency change of the QCM and by UV-visible spectroscopy. The results obtained showed a good coverage of the metal surface.

These QCMs showed good sensitivities to different volatile organic compounds (VOCs), with a low saturation limit. Enantiodiscrimination studies were carried out in the solid state by exposure of the functionalized QCMs to vapors of some enantiomeric pairs. While we did not observe chiral discrimination in the case of menthol, ephedrine, and 1,2-DACy, we obtained a remarkable degree of selectivity in the case of limonene. This result is particularly encouraging for the development of sensor arrays to be exploited in the analysis of real matrices in which chiral VOCs play an important role.

Experimental Section

Instrumentation: ^1H NMR spectra were recorded with Bruker AC300P (300 MHz) or Bruker AM400 (400 MHz) spectrometers. Chemical shifts are given in ppm relative to tetramethylsilane (TMS). Routine UV-visible spectra were measured on a Varian Cary 50 spectrophotometer, whereas more delicate measurements were performed on a Perkin–Elmer λ spectrophotometer equipped with a temperature-controlled cell holder. CD spectra were recorded on a JASCO J600 spectropolarimeter; all spectra, averaged over eight consecutive scans, were reported as molar ellipticity ($\text{degrees cm}^2 \text{d mol}^{-1}$). Mass spectra (FAB) were recorded on a VG Quattro spectrometer with *m*-nitrobenzyl alcohol (NBA, Aldrich) as a matrix in the positive ion mode.

Materials: Silica gel 60 (70–230 mesh) was used for column chromatography. Reagents and solvents (Aldrich, Merck, or Fluka) were of the highest grade available and were used without further purification. Solvents used for the spectrophotometric measurements, acetonitrile and chloroform Uvasol (Merck), were stored over activated molecular sieves.

UV-visible spectroscopy studies in solution: UV-visible spectroscopic studies of the interactions of chiral analytes with $[\text{Co}_2(\mathbf{1})]$ in solution were carried out in chloroform by following the absorbance changes in the 350–450 nm range (porphyrin derivative Soret band) upon guest complexation ($T = 25^\circ\text{C}$).

UV-visible spectroscopic titration: A typical procedure is as follows: aliquots of titrating solution of the guest (1×10^{-2} – 1×10^{-3} M), prepared by dissolving the required amount of olefin in a freshly prepared solution of $[\text{Co}_2(\mathbf{1})]$ (1 – 5×10^{-6} M) in chloroform, were added portionwise with a micro syringe to the diad solution (2.5 mL, 1 cm quartz cell, 25.0°C). The absorbance variation (Soret band) was monitored at different concentrations of added guest. The stability constants (K) were calculated by using a standard equation for a 1:1 complexation:^[28] $\Delta A = \Delta\epsilon[[\text{Co}_2(\mathbf{1})]]K[\text{G}]/(1 + K[\text{G}])$, where $\Delta A = A_0 - A_t$; $\Delta\epsilon = \epsilon_0 - \epsilon_{sc}$; $[\text{G}]$ is the concentration of the added guest. The computer aided nonlinear least-square fitting analyses were performed with the program Kaleidagraph[®] to give K and $\Delta\epsilon$. The experiments were run in duplicate and were reproducible within the range of 2–5%. Analyses carried out at different wavelengths (i.e., 412 and 435 nm) gave results in good agreement within 15%.

5-(4-Carboxyphenyl)-10,15,20-triphenylporphyrin (2): A solution of pyrrole (14.5 g, 0.21 mol) in acetic acid (100 mL) was added dropwise to a solution of 4-carboxybenzaldehyde (8.1 g, 0.054 mol) and benzaldehyde (20 g, 0.19 mol) in refluxing acetic acid (250 mL), over a period of 30 minutes. The reaction mixture was stirred at reflux temperature for an additional 3 h, then cooled to room temperature and left standing overnight. The crystalline residue, separated from the bulk solution, was collected by filtration, washed with methanol, and then purified by chromatography on SiO_2 . The first elution with CHCl_3 gave the 5,10,15,20-tetraphenylporphyrin (H_2TPP) co-product as a purple band, while the desired porphyrin was subsequently eluted with a 2% methanol/chloroform mixture, to give **2** (0.5 g, 0.76 mmol, 1.4% yield) as a purple crystalline solid. Another crop of product was obtained from the mother liquor as follows: the solvent was evaporated under reduced pressure and the black tarry residue dissolved in 200 mL of CHCl_3 . A saturated solution of aqueous NaHCO_3 was added to the mixture that was left stirring until the evolution of gas ceased. The separated organic layer was washed with a 10% aqueous Na_2CO_3 solution (3×200 mL) and then with brine until neutrality. To remove polymeric byproducts, silica gel (200 g) was added to the solution, and the resulting mixture stirred for 30 minutes. The solid mass was washed with CHCl_3 (1% MeOH) until a UV/vis check run showed the disappearance of the typical porphyrin absorption band ($\lambda = 419$ nm) of the product **2** in the eluate. The washings were collected, reduced to a small volume by rotary evaporation, and purified by chromatography on SiO_2 , first by eluting with CHCl_3 to recover H_2TPP and then with a 2% methanol/chloroform mixture to obtain the title porphyrin **2** (3 g, 4.5 mmol, 9% total yield). Spectroscopic characterization was in perfect agreement with data reported in the literature.^[29]

4,5-Bis[5-(4-carboxyphenyl)-10,15,20-triphenylporphyrinyl]-*trans*-1,2-dithiane (1): All manipulations were carried out under an inert atmosphere by using standard Schlenk techniques. Porphyrin **2** (50 mg, 0.076 mmol) was dissolved in dry and distilled CH_2Cl_2 (20 mL) in a 100 mL two-necked round-bottomed flask. An excess of a 2 M solution of oxalyl chloride (3 mL,

6 mmol) was added to the reaction mixture under stirring. After 2 h the solvent was evaporated in vacuo to give a dark brown residue, which was then dissolved in dry CH_2Cl_2 (20 mL). A solution of *trans*-1,2-dithiane-4,5-diol (5.8 mg, 0.38 mmol) in dry CH_2Cl_2 (4 mL) was rapidly added along with two drops of anhydrous pyridine. The mixture was left stirring overnight. The solvent was then stripped off in vacuo, and the residue dissolved in CH_2Cl_2 (20 mL), washed with brine, and dried (Na_2SO_4). The solvent was reduced to a small volume, and the residue was purified by chromatography (SiO_2), eluting with CH_2Cl_2 in order to give the title diporphyrin **1** (0.03 mmol, 0.043 g, 40% yield). The unreacted **2** was recovered by elution with a $\text{CH}_2\text{Cl}_2/\text{MeOH}$ 2% mixture. ^1H NMR (300 MHz, CDCl_3 , 25°C): $\delta = -2.71$ (brs, 4H), 3.24 (brs, 4H), 3.95 (brm, 2H), 7.60 (m, 20H), 8.06 (m, 18H), 8.71 (m, 16H); UV/Vis (CH_2Cl_2): $\lambda_{\text{max}} = 419, 513, 551, 589, 649$ nm; MS (FAB): m/z : 1435; elemental analysis calcd (%) for $\text{C}_{94}\text{H}_{64}\text{N}_8\text{O}_4\text{S}_2$: C 78.75, H 4.50, N 7.82; found: C 78.99, H 4.39, N 7.74.

Metalation reactions: The general procedure for the synthesis of the Co derivatives of the above porphyrins was as follows: a CHCl_3 solution of the substrate was placed in a round-bottomed flask equipped with a reflux condenser and a nitrogen inlet tube. The mixture was brought to reflux temperature and then an excess of a saturated methanolic solution of $\text{Co}(\text{OAc})_2$ (2 mL) was added under stirring. The progress of the reaction was monitored by UV-visible spectroscopy. At the end of the reaction the mixture was allowed to cool to room temperature, and the solvent was removed in vacuo. The residue was dissolved in CHCl_3 (50 mL), washed with brine (3×50 mL), and dried (Na_2SO_4). The solvent was removed in vacuo, and the residues, that is, the metalated porphyrins, were subsequently purified by crystallization from CH_2Cl_2 /hexane mixture.

[Co(2)]: Starting from **2** (0.8 g, 1.5 mmol), we obtained $[\text{Co}(\mathbf{2})]$ (1.04 g, 1.4 mmol, 93% yield) as a purple crystalline solid. UV/Vis (CH_2Cl_2): $\lambda_{\text{max}} = 412, 529, 554$ nm; MS (FAB): m/z (%): 716; elemental analysis calcd (%) for $\text{C}_{45}\text{H}_{28}\text{N}_4\text{O}_2\text{Co}$: C 75.52, H 3.94, N 7.83; found: C 75.40, H 3.89, N 7.77.

[Co(1)]: Starting from **1** (50 mg, 0.07 mmol) we obtained $[\text{Co}_2(\mathbf{1})]$ (46 mg, 0.03 mmol, 45% yield). UV/Vis (CH_2Cl_2): λ_{max} ($\log \epsilon$) = 412 (4.95), 435 (5.1), 548 (4.11), 590 (3.78) nm; MS (FAB): m/z (%): 1548; elemental analysis calcd (%) for $\text{C}_{94}\text{H}_{60}\text{N}_8\text{O}_4\text{S}_2\text{Co}_2$: C 72.96, H 3.91, N 7.24; found C 72.88, H 3.93, N 7.19.

Monolayer of [Co(3)]: A quartz microbalance (QCM) disk was dipped into a solution of 4-mercaptophenol (12.6 mg) in dichloromethane (100 mL) and left standing for 12 h. The disk was then rinsed with CH_2Cl_2 and dipped in a 10^{-3} M (0.07 mmol, 0.05 g in 70 mL of CH_2Cl_2) solution of the corresponding acyl chloride of **2** in CH_2Cl_2 . After standing for 1 day, the quartz disk was washed with CH_2Cl_2 , sonicated in CH_3OH , washed again with CH_2Cl_2 , and dried under N_2 .

Monolayer of [Co(1)] (Method 1 or one-step method): The QCM disk was dipped into a 10^{-3} M CH_2Cl_2 solution of $[\text{Co}_2(\mathbf{1})]$ (0.046 g, 0.03 mmol, 30 mL) for 12 h and then washed with CH_2Cl_2 , sonicated in CH_3OH , washed again with CH_2Cl_2 , and dried under a stream of N_2 .

Monolayer of [Co(1)] (Method 2 or two-step method): The quartz disk was dipped into a 10^{-3} M CH_2Cl_2 solution of *trans*-1,2-dithiane-4,5-diol (7 mg, 0.05 mmol, 50 mL) for 12 h before being washed with CH_2Cl_2 and again dipped into a 10^{-3} M solution of the corresponding acyl chloride of **2** for 12 h. The QCM disk was finally cleaned as reported above.

Sensor measurements: QCM sensors were AT-cut quartz crystals resonating at a fundamental frequency of 10 MHz. Frequency readout and electronic conditioning were performed with an electronic oscillating circuit, whose frequency was measured by a frequency counter (HP53131A). The frequency counter was connected, through a GP-IB link, with a PC that was set to supervising the measurement and collecting the sensor responses.

Eight sensors were housed in a 10 mL measurement chamber. In the case of triethylamine, saturated vapours of the analyte were obtained by bubbling N_2 into liquid amine; these vapours were diluted to different concentrations by a mass flow controller, with dry synthetic air as the carrier gas, and allowed to flow into the measurement chamber. The measurements were carried at a constant temperature (308 K), controlled by a Julabo F40 thermostat. Vapour-phase concentrations of the analyte were calculated by the Antoine equation.^[30]

In the case of chiral compounds a different experimental protocol had to be followed, owing to both the lower amount and the low volatility of these analytes. In this case a sealed vial containing the analyte was opened into a

2 L flask held at the constant temperature of 308 K. No significant variations of the headspace composition were observed after 1 h, as checked by GC analysis. Vapour-phase concentrations, calculated by the Antoine equation, were in good agreement with those measured by GC (internal standard dodecane). The headspace was then pumped into the measurement chamber by a micro pump at a constant flow rate of 0.2 L min⁻¹. The equilibrium response time for the sensors was in the order of 1 minute; after each measurement the chamber was purged by a flow of dry synthetic air. Typical sensor response is shown in Figure 6.

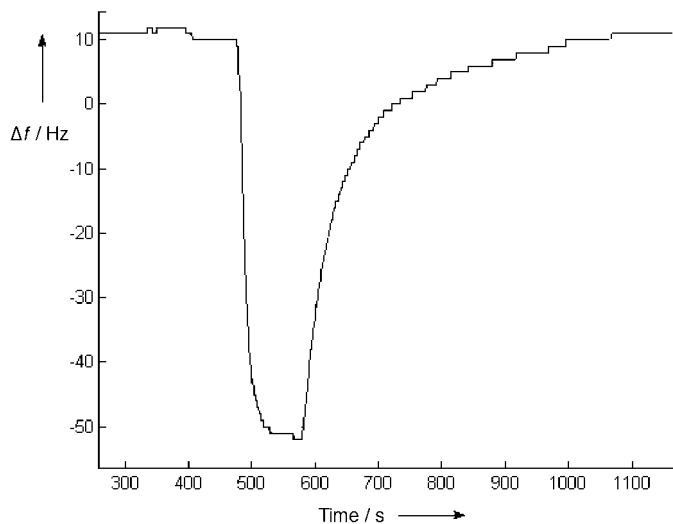


Figure 6. Typical frequency changes of a [Co₂(1)]-modified QCM sensor upon exposure to VOCs.

Acknowledgement

This work was supported by CNR MADESS II project 00.00781PF48.

- [1] a) A. Ulman, *An Introduction to Ultrathin Organic Films: From Langmuir–Blodgett to Self-Assembly*, Academic Press, San Diego, **1991**; b) A. Ulman, *Chem. Rev.* **1996**, *96*, 1533.
- [2] a) J. H. Fendler, *Chem. Mater.* **1996**, *8*, 1616; b) A. Kumar, G. M. Whitesides, *Science* **1994**, *263*, 60; c) *Nanoparticles and Nanostructured Films* (Ed.: J. H. Fendler), Wiley-VCH, Weinheim, **1998**.
- [3] W. Göpel, K. D. Schierbaum in *Sensors, Vol. 2* (Eds.: W. Göpel, T. A. Jones, M. Kleitz, J. Lundström, T. Seiyama), Wiley-VCH, Weinheim, **1991**, p. 1.
- [4] a) J. A. J. Brunink, C. Di Natale, F. Bungaro, F. A. M. Davide, A. D'Amico, R. Paolesse, T. Boschi, M. Faccio, G. Ferri, *Anal. Chim. Acta* **1996**, *325*, 53; b) C. Di Natale, A. Macagnano, G. Repole, A. D'Amico, R. Paolesse, T. Boschi, *Mater. Sci. Eng. C* **1998**, *5*, 209; c) C. Di Natale, R. Paolesse, A. Macagnano, V. I. Troitsky, T. S. Berzina, A. D'Amico, *Anal. Chim. Acta* **1999**, *384*, 249; d) C. Di Natale, R. Paolesse, A. Macagnano, A. Mantini, C. Goletti, A. D'Amico, *Sens. Actuators B* **1998**, *52*, 162; e) A. D'Amico, C. Di Natale, R. Paolesse, A. Macagnano, A. Mantini, *Sens. Actuators B* **2000**, *65*, 209; f) C. Di Natale, R. Paolesse, A. Macagnano, A. Mantini, P. Mari, A. D'Amico, *Sens. Actuators B* **2000**, *68*, 319; g) M. Andersson, M. Holmberg, I. Lundström, A. Lloyd-Spez, P. Mårtensson, R. Paolesse, C. Falconi, C. Di Natale, A. D'Amico, *Sens. Actuators B*, in press.
- [5] A. D'Amico, C. Di Natale, A. Macagnano, F. Davide, A. Mantini, E. Tarizzo, R. Paolesse, T. Boschi, *Biosens. Bioelectron.* **1998**, *13*, 711.
- [6] *The Porphyrin Handbook* (Eds.: K. M. Kadish, K. M. Smith, R. Guilard), Academic, **2000**.
- [7] a) J. E. Hutchison, T. A. Postlethwaite, R. W. Murray, *Langmuir* **1993**, *9*, 3277; b) J. Zak, H. Yuan, M. Ho, L. K. Woo, M. D. Porter, *Langmuir* **1993**, *9*, 2772; c) T. Akiyama, H. Imahori, Y. Sakata, *Chem. Lett.* **1994**, 1447; d) L.-H. Guo, G. McIendon, H. Razafitrimo, Y. L. Gao, *J. Mater. Chem.* **1996**, *6*, 369; e) W. Han, S. Li, S. M. Lindsay, D. Gust, T. A. Moore, A. L. Moore, *Langmuir* **1996**, *12*, 5742; f) H. Imahori, H. Norieda, S. Ozawa, K. Ushida, H. Yamada, T. Azuma, K. Tamaki, Y. Sakata, *Langmuir* **1998**, *14*, 5335; g) T. A. Postlethwaite, J. E. Hutchison, K. W. Hatchcock, R. W. Murray, *Langmuir* **1995**, *11*, 4109; h) J. E. Hutchison, T. A. Postlethwaite, C.-H. Chen, K. W. Hatchcock, R. S. Ingram, W. Ou, R. W. Linton, R. W. Murray, *Langmuir* **1997**, *13*, 2143; i) D. L. Pilloud, C. C. Moser, K. S. Reddy, P. L. Dutton, *Langmuir* **1998**, *14*, 4809; j) D. A. Offord, S. B. Sachs, M. S. Ennis, T. A. Eberspacher, J. H. Griffin, C. E. D. Chidsey, J. P. Collman, *J. Am. Chem. Soc.* **1998**, *120*, 4478; m) D. T. Gryko, C. Clausen, J. S. Lindsey, *J. Org. Chem.* **1999**, *64*, 8635; n) Z. Zhang, R. Hu, Z. Liu, *Langmuir* **2000**, *16*, 1158; o) Z. Zhang, S. Hou, Z. Zhu, Z. Liu, *Langmuir* **2000**, *16*, 537; p) N. Kanayama, T. Kanbara, H. Kitano, *J. Phys. Chem. B* **2000**, *104*, 271.
- [8] R. Paolesse, C. Di Natale, A. Macagnano, F. Davide, T. Boschi, A. D'Amico, *Sens. Actuators B* **1998**, *47*, 70.
- [9] J. D. Rawns, *Biochemistry*, Patterson, Burlington, **1989**.
- [10] a) J.-M. Lehn, *Supramolecular Chemistry*, Wiley-VCH, Weinheim, **1995**; b) *Comprehensive Supramolecular Chemistry Vol. 2* (Eds.: J.-M. Lehn, J. L. Atwood, J. E. D. Davies, D. D. MacNicol, F. Vögtle), Pergamon, Oxford, **1996**.
- [11] a) P. Schreier, A. Bernreuther, M. Huffer, *Analysis of Chiral Organic Molecules: Methodology and Applications*, de Gruyter, Berlin, **1995**, p. 371; b) J. Snopek, E. Smolkova-Keulemansova, T. Cserhati, K. Gahm, A. Stalcup in *Comprehensive Supramolecular Chemistry, Vol. 3* (Eds.: J.-M. Lehn, J. L. Atwood, J. E. D. Davies, D. D. MacNicol, F. Vögtle, T. Szejtli, T. Osa), Pergamon, New York, **1996**, p. 515.
- [12] a) J. Ide, T. Nakamoto, T. Moriizumi, *Sens. Actuators A* **1995**, *49*, 73; b) K. Bodenhöfer, A. Hierlmann, J. Seemann, G. Gauglitz, B. Koppenhoefer, W. Göpel, *Nature* **1997**, *387*, 577; c) K. Bodenhöfer, A. Hierlmann, J. Seemann, G. Gauglitz, W. Göpel, *Anal. Chem.* **1997**, *69*, 3058; d) K. Bodenhöfer, A. Hierlmann, M. Juza, V. Schurig, W. Göpel, *Anal. Chem.* **1997**, *69*, 4017; e) I. P. May, M. P. Byfield, M. Lindström, L. F. Wüschel, *Chirality* **1997**, *9*, 225.
- [13] C. Di Natale, A. Macagnano, F. Davide, A. D'Amico, R. Paolesse, T. Boschi, M. Faccio, G. Ferri, *Sens. Actuators B* **1997**, *44*, 521.
- [14] K. C. Persaud, G. Dodd, *Nature* **1982**, *299*, 352.
- [15] *Sensors and Sensory Systems for an Electronic Nose* (Eds.: J. W. Gardner, P. N. Bartlett), Kluwer Academic, Dordrecht (NL), **1992**.
- [16] W. Göpel, *Sens. Actuators B* **1998**, *52*, 125.
- [17] A. D'Amico, C. Di Natale, R. Paolesse, *Sens. Actuators B* **2000**, *68*, 324.
- [18] J. W. Buchler in *The Porphyrins* (Ed.: D. Dolphin), Academic Press, New York, **1978**, p. 389, and references therein.
- [19] For some recent reports on this topic see: a) J. M. Ribó, J. M. Bofill, J. Crusats, R. Rubires, *Chem. Eur. J.* **2001**, *7*, 2733; b) R. Rubires, J.-A. Ferrera, J. M. Ribó, *Chem. Eur. J.* **2001**, *7*, 436.
- [20] a) C. A. Hunter, J. K. M. Sanders, *J. Am. Chem. Soc.* **1990**, *112*, 5525; b) H.-J. Schneider, M. Wang, *J. Org. Chem.* **1994**, *59*, 7464.
- [21] Although an excellent adherence of the experimental points to a 1:1 binding curve is evident, the relative values could probably be the result of a series of consecutive conformational and binding equilibria. Detailed studies, which are beyond the immediate scope of this work, are in progress, and the results will be reported elsewhere.
- [22] For a recent overview on the chiral recognition of porphyrin derivatives see: a) H. Ogoshi and T. Mizutani, *Acc. Chem. Res.* **1998**, *31*, 81; b) X. Huang, K. Nakanishi, N. Berova, *Chirality* **2000**, *12*, 237.
- [23] F. Sauerbrey, *Zeit. Physik.* **1959**, *155*, 206.
- [24] A. Sgarlata, A. Angelaccio, N. Motta, R. Paolesse, C. Di Natale, A. D'Amico, *Surf. Sci.* **2000**, *466*, 167.
- [25] R. F. Pasternack, P. R. Huber, P. Boyd, G. Engasser, L. Francesconi, P. Fasella, G. Cerio Venturo, L. deC. Hinds, *J. Am. Chem. Soc.* **1972**, *94*, 4511.
- [26] M. Nappa, J. S. Valentine, *J. Am. Chem. Soc.* **1978**, *100*, 5075.
- [27] S. Brunauer, P. H. Emmet, E. Teller, *J. Am. Chem. Soc.* **1938**, *60*, 309.
- [28] K. A. Connors, *Binding Constants—The Measurements of Molecular Complex Stability*, Wiley, New York, **1987**.
- [29] a) S. Matile, N. Berova, K. Nakanishi, S. Novkova, I. Philipova, B. Blagoev, *J. Am. Chem. Soc.* **1995**, *117*, 7021; b) C. E. Kibbey, M. E. Meyerhoff, *Anal. Chem.* **1993**, *65*, 2189.
- [30] J. Riddick, A. Bunger in *Techniques of Chemistry, Vol. II* (Ed.: A. Weissberger), Wiley Interscience, New York, **1970**.

Received: June 15, 2001
Revised: January 14, 2002 [F3339]